BUTTERWORTH HEINEMANN

Investigation of the effect of a smooth strip on rough-wall turbulent boundary layers

Walid Chakroun
Kuwait University, Mechanical Engineering Department, Safat, Kuwait

Robert Taylor and Mesfin Medhin
Thermal and Fluid Dynamics Laboratory, Mechanical Engineering Department, Mississippii State University, Mississippi State, MS, USA

A series of experiments was conducted to study the effects of a smooth strip on heat transfer and fluid dynamics in the turbulent boundary layer on an otherwise rough surface. The first 0.9 m of the test section is rough, followed by 0.1-m smooth strip, and the remaining 1.4 m is rough. The rough surface is composed of 1.27-mm diameter hemispheres spaced 2-diameters apart in staggered arrays. The experiments include measurements of Stanton number distributions as well as mean temperature, mean velocity, and turbulence intensity profiles. The results are compared with previously published data from experiments with a rough leading portion and a smooth final portion and from experiments on an all-rough surface. Over the smooth strip, Stanton number decreases by almost 45% relative to the all-rough value; however, the Stanton number distribution recovers typical rough-wall behavior in a short distance. The Stanton number measurements are compared with predictions using the discrete-element method. In general, the agreement is excellent. Mean velocity and turbulence intensity profiles show the flow downstream of the strip to rapidly attain rough-wall behavior in the near region, while requiring more distance to exhibit a complete rough-wall behavior.

Keywords: rough wall; smooth strip; turbulent; boundary layer

Introduction

The effect of a smooth strip on the rough-wall turbulent boundary layer is investigated in this paper. Heat transfer and fluid dynamics experiments are performed, and the results are compared with the results from experiments on an all-rough and rough-to-smooth surfaces under equivalent flow conditions and with discrete-element boundary-layer computations.

The motivation for this work is concern over the results obtained when using smooth heat flux gauges on otherwise rough gas turbine blades. Taylor (1990) reported measurements of the surface roughness on in-service gas turbine blades and found the average roughness to range from about 1.5 μm to about 10 μm. This is very rough considering that the thickness of the boundary layer is on the order of 1 mm. Of special interest to this work are the Space Shuttle main engine fuel pump turbine blades, which Taylor et al. (1991) found to have rms roughness of about 15 μm. Tests on engine components are often conducted by installing small heat flux gauges, which are usually much smoother than the surrounding surface.

Antonio and Luxton (1971a, 1971b, 1972) studied the effects of a smooth-to-rough transition where the rough surface was composed of two-dimensional (2-D) ribs with the bases of the ribs aligned with the smooth section. They presented detailed datasets for velocity, turbulence, and skin friction measurements for both smooth-to-rough and rough-to-smooth cases. Schofield (1975) presented extensive flow measurements for step changes in surface roughness with adverse pressure-gradient. Prediction methods based on numerical solutions of the boundary-layer equations have been presented by Antonia and Wood (1975). Andreopoulous and Wood (1982) reported fluid mechanics results for flow over a smooth surface that was roughened using sand paper in one narrow strip at about midplate. However, there have been very few investigations reported for heat transfer.

Taylor et al. (1991) reported heat transfer data for the case where the first 0.9 m of the test section was rough, and the remainder was smooth. These experiments are referred to in this text as rough-to-smooth. Over the rough portion, a high

Address reprint requests to Dr. W. Chakron, Mechanical Engineering Department, P.O. Box 5969, Safat 13060, Kuwait.

Received 13 April 1994; accepted 14 February 1995

Int. J. Heat and Fluid Flow 16: 163–170, 1995

655 Avenue of the Americas, New York, NY 10010

0142-727X/95/$10.00
SSDI 0142-727X(95)00013-G

level of heat transfer typical for the level of roughness was observed. Downstream of the interface between the rough and the smooth portions, the Stanton number undergoes an immediate drop to a value at or below the equivalent smooth-wall Stanton number at the same x-Reynolds number.

Taylor and Chakroun (1993) presented heat transfer measurments and predictions for a short strip of roughness on an otherwise smooth surface. A short, rough strip was shown to have a significant influence on heat transfer and fluid flow. The Stanton number and skin-friction coefficient were greatly increased over the rough strip, but they dropped abruptly to values at or below the equivalent smooth-wall values just downstream of the roughness. In a short distance, the distributions recovered typical smooth-wall behavior.

The experiments reported herein consist of heat transfer and temperature profile measurements, as well as measurements of velocity and turbulent intensity profiles. The Stanton number measurements are compared with predictions using the discrete-element method. The experimental results are compared with the results of Taylor et al. (1991) for the case of a step change in surface roughness from rough-to-smooth and the all-rough experiments of Hosni et al. (1991). The same rough surface was used in all experiments.

Experimental apparatus and techniques

The experiments are performed in the Turbulent Heat Transfer Test Facility (THTTF). This facility, as shown schematically in Figure 1, is a closed-loop wind tunnel with a freestream velocity range of 5–67 m/s. A brief description of the apparatus is given below. A more detailed discussion of the facility and its qualification can be found in Coleman et al. (1988) and Hosni et al. (1991).

The bottom wall of the nominally 2.4-m long by 0.5-m wide by 0.1-m high test section consists of electrically heated

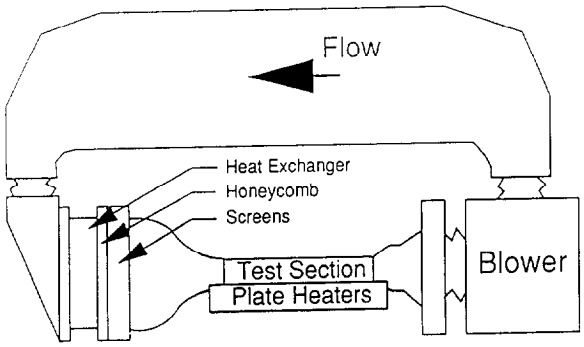

Figure 1 Schematic of Turbulent Test Facility (THTTF)

nickel-plated aluminum plate (about 10-mm thick by 0.1 m in the flow direction) butted together to form a continuous flat surface. The rough test plates considered here are precision machined and have 1.27-mm diameter hemispherical elements spaced 2-diameters apart in staggered arrays, as shown in Figure 2.

Figure 3a is a schematic diagram for the test section used in these experiments. The first 0.9 m of the test surface is rough, the next 0.1 m is smooth, and the remaining 1.4 m is rough. All the rough plates are 10-cm wide. The smooth strip is composed of 4 smooth plates, each 2.5-cm wide. These are installed to give better resolution of the Stanton number behavior after the step. Figure 3b shows the rough-to-smooth test surface used by Taylor et al. (1991), and mentioned previously, with 0.9 m roughened with the hemispheres and the remaining 1.5 m smooth.

The top wall of the test section is made of plexiglass and can be adjusted to maintain a constant freestream velocity. The boundary layer is tripped at the exit of the 19:1 area-ratio

Notation

A	plate surface area
A^+	turbulence model damping parameter
C_D	local element drag coefficient
C_f	skin-friction coefficient
C_p	specific heat
d	local roughness element diameter
d_o	roughness element base diameter
H	time mean enthalpy
k	roughness element height
K	thermal conductivity
l_m	mixing length
L	roughness element spacing
Nu_d	local element Nusselt number
P	pressure
Pr	Prandtl number
q_c	conductive heat loss rate
q_r	radiative heat loss rate
r	recovery factor
Re_d	local element Reynolds number
St	Stanton number
T	local fluid static temperature
T_∞	freestream static temperature
T_o	freestream total temperature
T_r	freestream recovery temperature
T_{rail}	side rail temperature
T_w	wall (plate) temperature
T_R	roughness element temperature
u	mean longitudinal velocity
u'	longitudinal velocity fluctuation
u^*	friction velocity
u^+	nondimensional velocity, u/u^*
U_∞	local freestream velocity
$(UA)_{\mathrm{eff}}$	effective overall conductance
v	surface normal velocity
W	plate heater power
x	axial distance from nozzle exit
y	coordinate normal to the wall surface
y^+	nondimensional y, $\rho y u^+/\mu$
z	transverse coordinate

Greek

β	blockage factors
Δ	thermal boundary-layer thickness
δ	boundary-layer thickness
ε	plate surface emissivity
μ	viscosity
ρ	density
σ	Stefan–Boltzmann constant

Subscripts

e	edge conditions
T	turbulent values
w	wall value
∞	freestream values

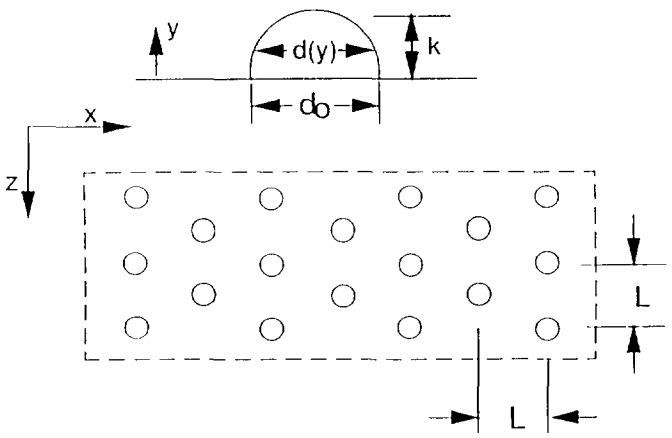

Figure 2 Surface roughness description

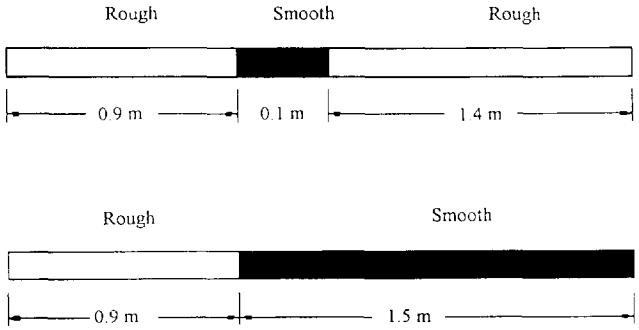

Figure 3 Schematic diagram of test surfaces

nozzle with a 1-mm × 12-mm wooden strip. This trip location is immediately in front of the heated surface.

Stanton number determination

The data-reduction expression for the Stanton number is as follows:

$$\mathrm{St} = \frac{W - (UA)_{\mathrm{eff}}(T_w - T_{\mathrm{rail}}) - \sigma \varepsilon A(T_w^4 - T_r^4)}{\rho C_p U_r A(T_w - T_0)} \tag{1}$$

The measurement techniques for all the variables in the Stanton number determination can be found in Coleman et al. (1988) and Hosni et al. (1991). The uncertainty in the experimentally determined Stanton number is estimated based on the ANSI/ASME Standard on Measurement Uncertainty (1986) following the procedures of Coleman and Steele (1989). For the Stanton number data in this paper, the overall uncertainty, as discussed by Hosni et al. (1991) and Taylor et al. (1991), ranges from ±2% to ±5% for the 10-cm wide plates, depending upon the flow conditions. For the 2.5-cm wide plates used for the smooth strip, the uncertainty in the Stanton number was found to be from ±3% to ±11%, depending upon the flow conditions.

Profile measurements

The profiles of mean velocity and the fluctuating longitudinal velocity component ($\overline{u'^2}$) are taken with a DANTEC 55P05 horizontal hot-wire. The traverse of the boundary-layer velocity profile begins with the probe starting just above the wall and moving upward. At each measurement position, 1,000 instantaneous anemometer output voltage readings 0.01 seconds apart are taken and converted into velocities using a fourth-order least-squares calibration equation. This sample size and sampling rate were chosen based on the work of George et al. (1978). The sampling size was chosen to achieve unbiased estimators of $\bar{u}$ and $\overline{u'^2}$. The sampling rate was chosen so that the sampling time is greater than twice the time scale of the flow. It was found that 1,000 readings 0.01 seconds apart gave consistent results for the present flow conditions. The overall uncertainties in the values of u and ($\overline{u'^2}$) were estimated by Coleman et al. (1988) to be ±2 and ±5%, respectively.

The mean temperature profiles are measured using a specially calibrated, butt-welded, chromel-constantan thermocouple probe. The overall uncertainty in the temperature measurement with this probe was quoted by Coleman et al. (1988) to be ±0.08°C.

Discrete-element roughness model

The major physical phenomena that distinguish flow over a rough surface are blockage of the flow, form drag on the roughness elements, and local heat transfer between the elements and the fluid. The following discrete-element equations result from applying the laws of conservation of mass, momentum, and energy to a control volume that considers blockage, form drag, and roughness element heat transfer (Taylor et al. 1984, 1985).

Continuity:

$$\frac{\partial}{\partial x}(\rho \beta_x u) + \frac{\partial}{\partial y}(\rho \beta_y v) = 0 \tag{2}$$

Momentum:

$$\beta_x \rho u \frac{\partial u}{\partial x} + \beta_y \rho v \frac{\partial u}{\partial y} = -\frac{\partial}{\partial x}(\beta_x P) + \frac{\partial}{\partial y}\left[\beta_y(\mu + \mu_T)\frac{\partial u}{\partial y}\right] - \tfrac{1}{2}\rho C_D \, \mathrm{d}(y) \frac{u^2}{L^2} \tag{3}$$

Energy:

$$\beta_x \rho u \frac{\partial H}{\partial x} + \beta_y \rho v \frac{\partial H}{\partial y} = \frac{\partial}{\partial y}\left[\beta_y \frac{K + K_T}{C_p}\frac{\partial H}{\partial y}\right] + u\frac{\partial}{\partial x}(\beta_x P) + \beta_y(\mu + \mu_T)\left(\frac{\partial \mu}{\partial y}\right)^2 + \frac{1}{2}\rho C_D \frac{\mathrm{d}(y)}{L^2} u^3 + \pi \frac{K Nu_d}{L^2}(T_R - T) \tag{4}$$

The terms β_x and β_y are the spatially averaged fractions of the control surfaces open to flow and are called the blockage factors. Taylor et al. (1984, 1989) have shown that for a uniform array, $\beta_x = \beta_y = 1 - (\pi d^2/4L^2)$, where d is the local element diameter at level y. These blockage factors can be computed directly from the surface description and require no empirical fluid mechanics input. The local drag is modeled via the local element drag coefficient C_D, and the local heat transfer is modeled via the local Nusselt number Nu_d. Empirical fluid mechanics and heat transfer input, in a manner similar to turbulence closure models, are required for these parameters.

The solution of Equations 2–4 requires a turbulence model for μ_T and K_T and a roughness model for C_D and Nu_d. The turbulence model used herein is not modified to include

roughness effects, because the physical effects of the roughness are included explicitly in the differential equations. The Prandtl mixing-length model with Van Driest damping and constant turbulent Prandtl number $Pr_T = 0.9$ are used in this study:

$$\mu_T = \rho \ell_m^2 \left| \frac{\partial u}{\partial y} \right| \tag{5}$$

where

$$\ell_m = 0.4y[1 - \exp(-y^+/A^+)],\ \ell_m < 0.09\delta$$
$$\ell_m = 0.09\delta, \quad \text{otherwise}$$
$$A^+ = 26$$

A lag model was used with the turbulence model at the rough-to-smooth interface and the smooth-to-rough interface. The local predicted eddy viscosity, μ_{Tv} was averaged in a weighted sense with an upstream reference viscosity μ_{To} at location x.

$$\mu_T = \mu_{T_o}(1 - \eta) + \mu_{T_v}\eta$$
$$\eta = 1 - e^{[-(x - x_0)]/\lambda)} \tag{6}$$

where $\lambda = 5\delta_o$ at the rough-to-smooth interface and $\lambda = \delta_o$ at the smooth-to-rough interface. In both cases x_o was located 0.02 m upstream of the interface.

Taylor et al. (1984) have calibrated a model for C_D and Hosni et al. (1991) for Nu_d in terms of the local element Reynolds number Re_d. The results of these calibrations are as follows:

$$\log_{10}(C_D) = -0.125 \log_{10}(Re_d) + 3.75,\ Re_d < 6 \times 10^4$$
$$C_D = 0.6,\ Re_d > 6 \times 10^4 \tag{7}$$

and

$$Nu_d = 1.7\, Re_d^{0.49}\, Pr^{0.4},\ Re_d < 13.8 \times 10^3$$
$$Nu_d = 0.0605\, Re_d^{0.84}\, Pr^{0.4}, \quad \text{otherwise} \tag{8}$$

The C_D model has been verified by comparisons with data for values of Re_d up to about 25,000. The Nu_d model has been verified by comparisons with data up to $Re_d \sim 2{,}500$.

The boundary conditions are applied at the smooth base wall ($y = 0$) and the free stream. At $y = 0$, $u = v = 0$, and $H = H_w$. As $y \to \infty$, $u \to U_\infty$, and $H \to H_\infty$.

The spatially averaged skin friction coefficient is as follows:

$$C_f = \frac{(\beta_y)_w \mu \left.\frac{\partial u}{\partial y}\right|_w + \frac{1}{2}\frac{1}{L^2}\int_0^k (\rho d C_D u^2)\mathrm{d}y}{\frac{1}{2}\rho_\infty U_\infty^2} \tag{9}$$

In the same vein, the spatially averaged Stanton number is

$$St = \frac{-(\beta_y)_w \frac{K}{C_p}\left.\frac{\partial H}{\partial y}\right|_w + \frac{\pi}{L^2}\int_0^k [(K\, Nu_d)(T_R - T)]\mathrm{d}y}{\rho_\infty U_\infty (H_w - H_{0,\infty})} \tag{10}$$

The results shown in this paper were obtained using a version of the Mississippi State University-developed instructional boundary-layer computer code, BLACOMP. BLACOMP is a 2-D, variable property laminar/turbulent boundary-layer computer code written in FORTRAN. Transition is simulated by defining the beginning and ending of the transition region and using an intermittency factor to model the transition region. Detailed information on BLACOMP is available in Gatlin and Hodge (1983, 1989). The discrete-element surface roughness model modification of BLACOMP follows closely the formulation of Taylor et al. (1984) and is straightforward.

Results

The data were obtained for zero-pressure gradient and constant wall temperature conditions and reduced under the assumption of incompressible turbulent boundary-layer flow. The data were collected for freestream velocities ranging from 6 m/s to 58 m/s. The corresponding plate-length Reynolds numbers range from 50,000 to 7,000,000. The x-Reynolds numbers immediately upstream of the smooth strip range from 340,000 to 3,100,000 and those immediately downstream of the smooth strip from 410,000 to 3,800,000.

Figures 4 through 8 present the heat transfer results for the smooth-strip experiments in terms of Stanton number distribution vs. x-Reynolds number for freestream velocities of 6 m/s, 12 m/s, 28 m/s, 43 m/s, and 58 m/s. The figures also include for comparison the results for the all-rough, rough-to-smooth, and all-smooth cases. The all-rough results are taken from Hosni et al. (1991), the rough-to-smooth results are taken from Taylor et al. (1991), and all-smooth results are taken from Coleman et al. (1988). All of these datasets were collected in the same facility using the same instrumentation and procedures. Therefore, all of the data contain many of the same bias errors and can be compared with a high degree of confidence. The figures for 12, 28, 43, and 58 m/s also show comparisons with predictions using the discrete-element roughness model.

The figures show the smooth strip has an immediate and large effect on heat transfer. For each of the freestream velocities, the Stanton number for the smooth-strip case follows the all-rough data upstream of the smooth strip, rapidly approaches the all-smooth data over the smooth strip, and increases back to the all-rough level once the wall again becomes rough. In most of the cases, the Stanton numbers immediately after the step change in roughness fall below the

* Turbulent flows that are influenced by surface roughness are usually divided into three regimes. Aerodynamically smooth flows and those where the roughness effects are so small that the flow behaves as if the wall were smooth. Fully rough flows are those where the roughness so dominates the momentum transport to the wall that viscous effects are negligible. In turbulent pipe flow, fully rough flows are those where the friction factor is no longer a function of the Reynolds number. Transitionally rough flows occur at Reynolds numbers in between, and both viscous and roughness effects are significant.

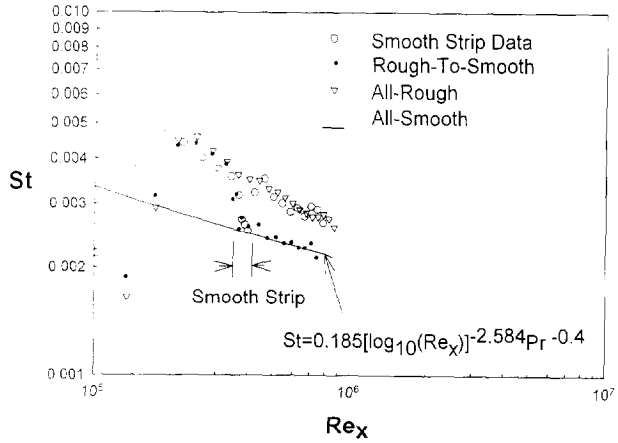

Figure 4 Comparison of the Stanton number data for the smooth strip, rough-to-smooth (Taylor et al. 1991), all-rough (Hosni et al. 1991), and smooth wall correlation (Coleman et al. 1988) with $U_\infty = 6$ m/s

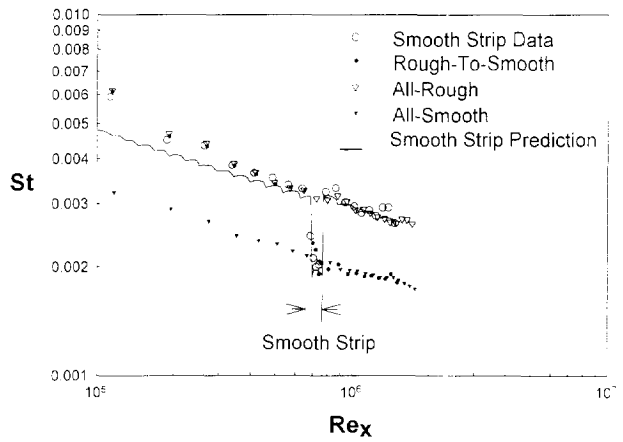

Figure 5 Comparison of the Stanton number data and predictions for the smooth strip, rough-to-smooth (Taylor et al. 1991), all-rough (Hosni et al. 1991), and all-smooth (Coleman et al. 1988) cases with $U_\infty = 12$ m/s

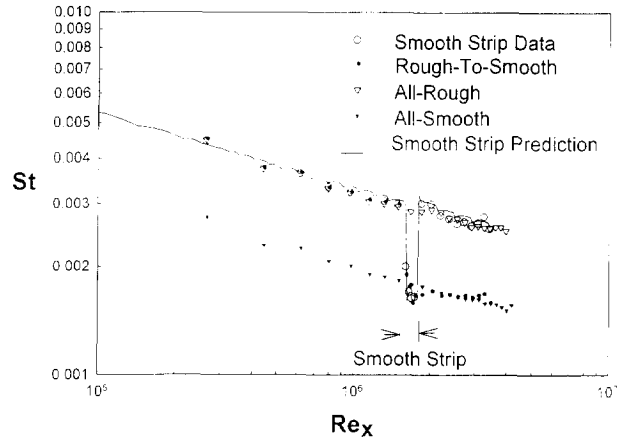

Figure 6 Comparison of the Stanton number data and predictions for the smooth strip, rough-to-smooth (Taylor et al. 1991), all-rough (Hosni et al. 1991), and all-smooth (Coleman et al. 1988) cases with $U_\infty = 28$ m/s

all-smooth data and rise back to or above the all-rough values immediately downstream of the smooth strip.

The 6-m/s case shown in Figure 4 behaves differently. Despite the trip at the nozzle exit and the rough surface, the flow remains laminar for a considerable length. The flow becomes fully turbulent at a Reynolds number of about 150,000, and a transitionally rough* boundary layer is established before the smooth strip interface. No all-smooth data are available for this velocity, so the data are compared with the smooth-wall correlation for turbulent boundary layers (Coleman et al. 1988). Over the smooth strip, the Stanton number decreases rapidly in a smooth, continuous fashion to the smooth-wall correlation. Downstream of the smooth strip where the wall becomes rough, the Stanton number also increases in a smooth continuous fashion to the all-rough value. A similar behavior in Stanton number distribution is observed over the first smooth plate for the rough-to-smooth case. After the step change in roughness, the Stanton number decreases in a continuous fashion to the new smooth wall condition.

Figure 5 shows the results for the 12-m/s case. For this case, there is no appreciable laminar region, because no transition from laminar to turbulent flow is observed, as in Figure 4. The Stanton number drops in an abrupt fashion or to below the all-smooth value, with the Stanton number appearing to dip below the equivalent smooth-wall values after the change in surface roughness. However, the uncertainty in the 0.025-m test-plate Stanton number is too large to draw a definite conclusion. Downstream of the smooth strip, an abrupt increase in Stanton number to or above the all-rough data is observed. There appears to be a slight overshoot; however, because of the uncertainty in the measurement, no definite conclusion can be drawn. Similar results over the first smooth plate from the rough-to-smooth experiments are observed. After the step change in roughness, the Stanton number for the rough-to-smooth case drops dramatically, undershooting the smooth-wall values and then increasing toward the new-smooth-wall equilibrium values.

Figures 6 through 8 show the data for the higher velocities. In all the figures, the Stanton number over the smooth strip behaves similarly to that over the first smooth plate from the rough-to-smooth data. The Stanton number decreases in an abrupt fashion to or below the all-smooth data. The dip in Stanton number below the all-smooth data is more pronounced

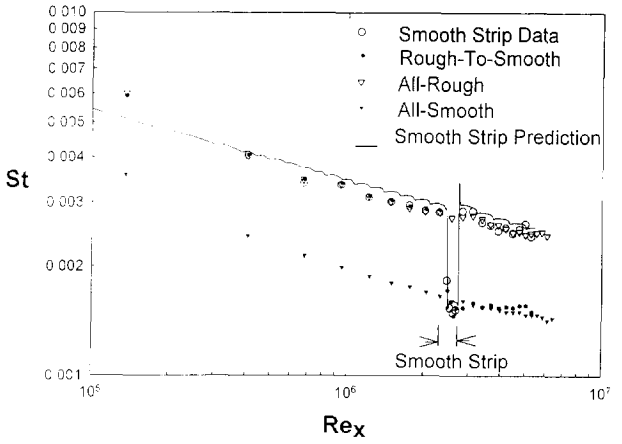

Figure 7 Comparison of the Stanton number data and prediction for the smooth strip, rough-to-smooth (Taylor et al. 1991), all-rough (Hosni et al. 1991), and all-smooth (Coleman et al. 1988) cases with $U_\infty = 43$ m/s

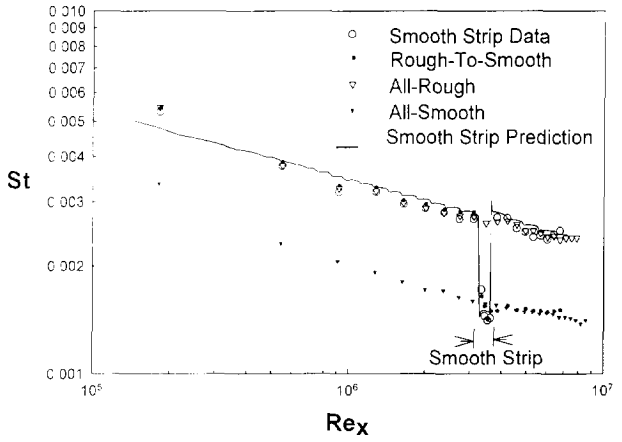

Figure 8 Comparison of Stanton number data and prediction for the Stanton number data and prediction for the smooth strip, rough-to-smooth (Taylor et al. 1991), all-rough (Hosni et al. 1991), and all-smooth (Coleman et al. 1988) case with $U_\infty = 58$ m/s

for higher velocities and is greater than the order of the uncertainty. The Stanton number for the smooth-strip case rises sharply, with a slight overshoot indicated at the smooth-to-rough interface. The Stanton numbers for rough-to-smooth experiments recover to the smooth-wall values.

The predictions for the 12 m/s, 28 m/s, 43 m/s, and 58 m/s are plotted on the corresponding figures for comparison. The predictions show excellent agreement with the experimental data. The predictions for the 12 m/s-case presented in Figure 5 show a deviation from the experimental data upstream of the smooth strip. Other than that, the prediction shows excellent agreement with the data. The predictions capture the drastic drop and rise in the Stanton numbers, including the overshoot at the smooth-to-rough interface.

The heat transfer results indicate that the use of smooth gauges on an otherwise rough surface is not appropriate and can lead to errors of 35–40%. Although the results obtained here are for a 2-D situation, they can still apply to the real situation with thee-dimensional (3-D) heat flux gauges, because 3-D boundary layers behave much like the 2-D boundary layers aligned with the local velocity vector in the near-wall region (White, 1974).

Figure 9 provides a composite plot of the boundary-layer mean velocity profiles taken with a hot-wire at a nominal freestream of 12 m/s plotted in y vs. u/U_∞ coordinates. Figure 10 shows an expanded scale of the lower portion of the data between $y = 0$ and $y = 1$ cm to help see the behavior of the velocity profiles close to the wall. In both figures, the u/U_∞ abscissa is plotted with a multiple origin to show the progression of the velocity profiles upstream, over, and downstream of the smooth strip. The plots also show the corresponding rough-to-smooth and all-rough velocity profiles under carefully matched flow conditions for the identical locations. The flow conditions are matched by establishing nearly identical thermal and freestream boundary conditions.

As expected, just upstream of the smooth strip at $x = 0.85$ m, the profiles for all three experiments are identical, because the wall for all three experiments is rough up to that location.

Downstream of the interface over the first smooth plate, the velocity profiles for the rough-to-smooth data deviate quickly from the all-rough data near the wall until about $y = 0.3$ cm, where the two profiles merge together. Farther downstream of the interface, the deviation from the rough wall increases until

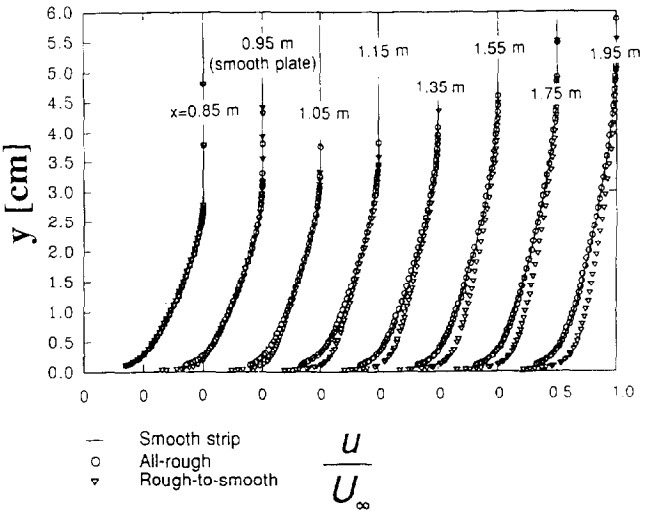

Figure 9 Velocity profiles for the smooth strip, rough-to-smooth, and all-rough cases at increasing locations plotted on a shifted axis for $U_\infty = 12$ m/s

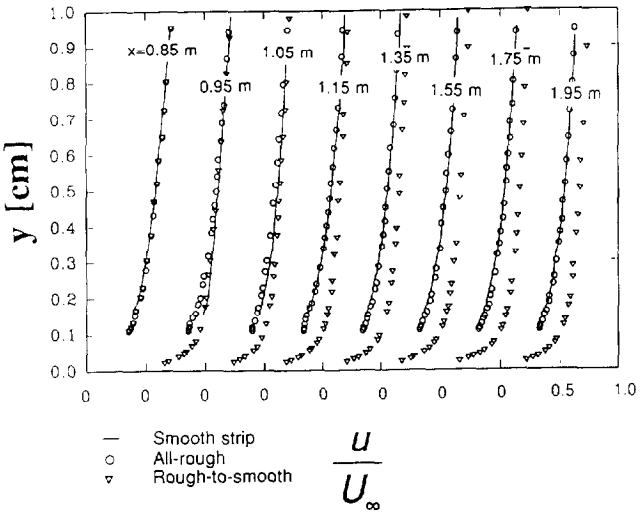

Figure 10 An extended scale of the near wall data for the velocity profiles for the smooth strip, rough-to-smooth, and all rough cases at increasing locations plotted on a shifted axis for $U_\infty = 12$ m/s

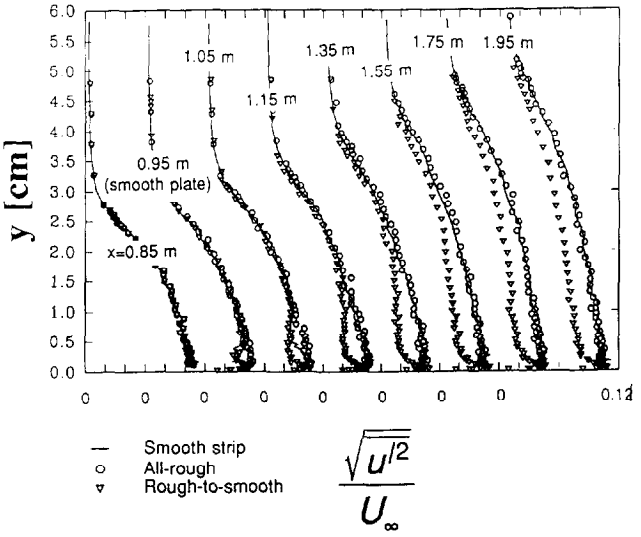

Figure 11 Turbulence intensity profiles for the smooth strip, rough-to-smooth, and all rough cases at increasing locations plotted on a shifted axis for $U_\infty = 12$ m/s

the fully smooth wall profile is obtained. An internal layer grows immediately downstream of the step because of the rapidly varying shear stress distribution. The flow outside the internal layer remains mostly unaffected by the change in surface roughness; whereas, the flow inside the internal layer assumes a smooth-wall characteristic.

For these measurements, the hot-wire probe was fitted with a keel appropriate for indexing the probe over the rough surface. Therefore, we could not get as close to the wall as in the rough-to-smooth case, but, clearly, the profiles for the two cases are similar over the smooth strip ($x = 0.95$ m). Downstream over the rough wall, the internal layer rapidly mixes, and the profiles recover to those of the all-rough experiments. The internal layer is not distinguishable in the mean velocity data.

Profiles of axial turbulence intensity are also determined with the horizontal hot-wire at the same locations as the mean velocity profiles. Figure 11 shows the turbulent intensity

profiles for a freestream velocity of 12 m/s plotted in coordinates y vs. $\frac{\sqrt{u'^2}}{U_\infty}$ on a multiple origin plot. An expanded-scale of the data between $y = 0$ and $y = 1$ cm is shown in Figure 12. Also shown on these plots are the all-rough (Hosni et al. 1991) and the rough-to-smooth (Taylor et al. 1991) profiles at the same x-locations.

Upstream of the interface, at the $x = 0.85$ m location, the turbulence intensity profiles for the all-rough, rough-to-smooth, and smooth strip cases are identical as expected.

Downstream of the interface, the near-wall regions of the rough-to-smooth profiles quickly deviate from the all-rough profiles. However, both profiles stay nearly identical in the outer region for a considerable distance. Similar to the velocity profiles, the turbulence intensity profiles outside the internal layer overlap the all-rough profiles and remain mostly unaffected by the change in surface roughness. Inside the internal layer, the turbulence intensity level assumes a smooth-wall characteristic.

Over the smooth strip ($x = 0.95$ m), the intensity profile for the smooth strip case is similar to that of the first smooth plate for the rough-to-smooth case. The turbulence profile deviates quickly from the all-rough profiles to the rough-to-smooth data in the near wall region up to $y = 0.7$ cm; however, both profiles stay nearly identical in the outer region. At the next downstream location $x = 1.05$ m, the turbulence intensity close to the wall is starting to recover to the all-rough values. Three regions can be identified at this location: very near the wall up to $y = 0.3$ cm there is a rough-wall dominated internal layer, an intermediate layer extends from $y = 0.3$ to $y = 1.1$ cm, where both smooth-wall and rough-wall influence is seen, and the outer region where the boundary layers continue to evolve as the original rough-wall boundary layer. At $x = 1.15$ m location, a remnant of the smooth-strip influence is still seen. At $x = 1.35$ m, the intermediate layer has washed out, and the profile resembles that of all the all-rough case.

Figure 13 shows plots of the nondimensional temperature profiles *versus* y/Δ for free-stream velocity of 12 m/s. The temperature profiles are measured at $x = 0.85$ m, 0.95 m (smooth strip), 1.05 m, and 1.15 m. Unfortunately, no temperature profiles were taken at stations farther downstream of the smooth plate. The profiles at $x = 1.05$ and 1.15 m do not

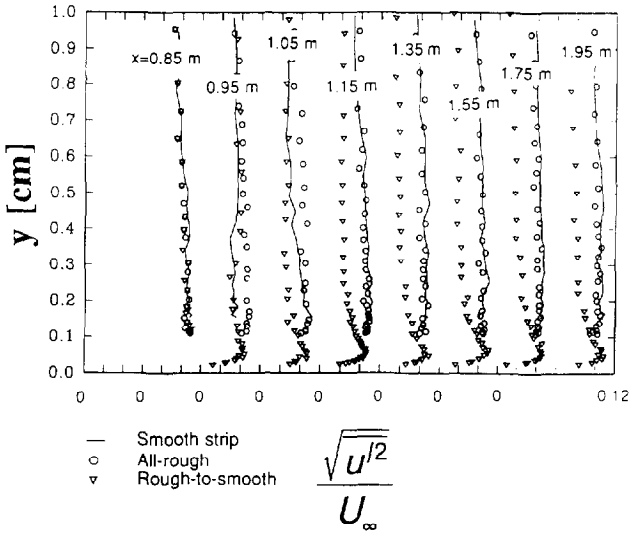

Figure 12 An extended scale of the near wall data for the turbulence intensity profiles for a smooth strip, rough-to-smooth, and all-rough cases at increasing locations plotted on a shifted axis for $U_\infty = 12$ m/s

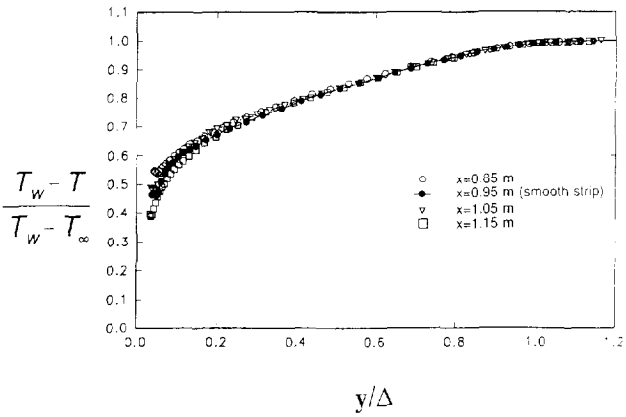

Figure 13 Mean temperature profiles before, over, and downstream of the smooth strip for $U_\infty = 12$ m/s

resemble immediately that of the rough plate in the region close to the wall.

The temperature, velocity, and turbulent intensity profiles provide a possible explanation for why the Stanton number drops dramatically after the rough-to-smooth interface. Over the rough surface, the temperature and velocity profiles are greatly retarded when compared with the smooth-wall profiles. However, over the rough surface the net heat transfer is greatly augmented by direct transfer to the protruding roughness elements. Hosni et al. (1991) estimate for full rough boundary layers with this rough surface that 65% of the net transfer is accounted for by direct transfer to the roughness elements, which account for only 33% of the total surface area. When these retarded profiles move over the smooth surface, they must rely on conduction through the boundary layer for all the heat transfer. If the gradients in the sublayer are retarded enough, the heat transfer rate will be less than that of an equivalent all-smooth boundary layer. The overshoots at the smooth-to-rough interface, where the Stanton numbers are larger than the all-rough values, are caused by the establishment of new internal layers at this interface.

Summary and conclusion

Heat transfer and fluid mechanics data are collected for zero-pressure gradient, incompressible, constant wall temperature air flow over a rough wall with a short smooth strip. The surface roughness is composed of hemispheres spaced 2-diameters apart in staggered arrays. The smooth strip is shown to have a large influence on heat transfer and fluid flow. Over the smooth strip, the Stanton number undergoes an immediate drop to a value at or below the equivalent smooth-wall value. In a distance of 0.2-m downstream of the smooth strip, the Stanton number distribution recovers typical rough-wall behavior. The comparison of the heat transfer results with predictions using the discrete-element method is excellent.

The results indicate that the use of smooth heat flux gauges to measure the heat transfer on an otherwise rough surface will give results that differ from the actual heat flux on the rough surface. The error induced by using smooth heat flux gauges on otherwise rough surfaces can reach 45%. Smooth gauges are not recommended for use on rough surfaces.

In the turbulence intensity profile measurements downstream of the smooth strip, three distinct layers are observed. In the outer region, the boundary layer continues to evolve as the original rough-wall boundary layer. At the intermediate

level, there is a smooth-wall-influenced internal layer. Very close to the wall there is a roughness dominated internal layer. After a distance of 0.4 m from the smooth-to-rough interface, the smooth strip influence washes out, and the profile resembles that of the all-rough.

References

Andreopoulous, J. and Wood, D. H. 1982. The response of a turbulent boundary layer to a short length of surface roughness. *J. Fluid Mech.*, **118**, 143–164

Anon. 1986, Measurement uncertainty, ANSI/ASME PTC 19.1-1985, Part 1, 1986

Antonia, R. A. and Luxton, R. E. 1971a. The response of a turbulent boundary layer to a step change in surface roughness. Part 1. Smooth-to-rough. *J. Fluid Mech.*, **48**, 721 726

Antonia, R. A. and Luxton, R. E. 1971b. The response of a turbulent boundary layer to an understanding step change in surface roughness. *J. Basic Eng.*, **93**, 22–23

Antonia, R. A. and Luxton, R. E. 1972. The response of a turbulent boundary layer to a step change in surface roughness. Part 2. Rough-to-smooth. *J. Fluid Mech.*, **48**, 721 726

Antonia, R. A. and Wood, D. H. 1975. Calculation of a turbulent boundary layer downstream of a small step change in surface roughness. *Aeronaut. Quarterly*, **26**, 202–210

Coleman, H. W., Hosni, M. H., Taylor, R. P. and Brown, G. B. 1988. Smooth wall qualification of a turbulent heat transfer test facility. Rep. TFD-88-2, Mechanical and Nuclear Engineering Department, Mississippi State University

Coleman, H. W. and Steele, W. G. 1989. *Experimentation and uncertainty analysis for engineers*, Wiley, New York

Gatlin, B. and Hodge, B. K. 1983. An instructional computer program for computing the steady, compressible turbulent flow of an arbitrary fluid near a smooth wall. Mechanical and Nuclear Engineering Department, Mississippi State University

Gatlin, B., and Hodge, B. K. 1989. A generalized program for computing two-dimensional boundary layers on a personal computer. Paper presented at the 25th ASME/AIChE National Heat Transfer Conference, Philadelphia, PA

George, W. K., Beuther, P. D. and Lumley, J. L. 1978. Processing of random signals. *Proc. Dynamic Flow Conf.* 757–800

Hosni, M. H., Coleman, H. W., and Taylor, R. P. 1991. Measurement and calculation of rough-wall heat transfer in the turbulent boundary layer. *Int. J. Heat Mass Transfer*. **34**, 1067–1082

Schofield, W. H. 1975. Measurements in adverse pressure-gradient turbulent boundary layers with a step change in surface roughness. *J. Fluid Mech.*, **70**, 573–593

Taylor, R. P. 1990. Surface roughness measurements on gas turbine blades. *J. Turbomach.*, **112**, 175–180

Taylor, R. P. and Chakroun, W. M. 1993. Heat transfer in turbulent boundary layer with a short strip of roughness. *J. Thermophysics and Heat Transfer*, **7**, 183–185

Taylor, R. P., Coleman, H. W. and Hodge, B. K. 1984. A discrete element prediction approach for turbulent flow over rough surfaces. Report TFD-84-1. Mechanical and Nuclear Engineering Department, Mississippi State University

Taylor, R. P., Coleman, H. W. and Hodge, B. K. 1985. Prediction of turbulent rough-wall skin friction using a discrete element approach. *J. Fluids Eng.*, **107**, 251–257

Taylor, R. P., Hodge, B. K. and Coleman, H. W. 1989. Prediction of heat transfer in turbulent flow over rough surfaces. *J. Heat Transfer*, **111**, 568–572

Taylor, R. P., Taylor, J. K., Hosni, M. H. and Coleman, H. W. 1991. Heat Transfer in the turbulent boundary layer with a step change in surface roughness. ASME Paper 91-GT-266, presented at the International Gas Turbine and Aeroengine Congress and Exposition, Orlando, FL, June 3–6

White, F. 1974. *Viscous Fluid Flow*, McGraw-Hill, New York